International Journal of Research in Engineering and Science (IJRES)
ISSN (Online): 2320-9364, ISSN (Print): 2320-9356
www.ijres.org Volume 7 Issue 6 ǁ June, 2019 ǁ PP. 32-36

Simulation of Weld Morphology During Friction Stir Welding of Aluminum- Stainless Steel Joint

DINESH KUMAR KINATHI
Lecturer, Mechanical Engineering.
Govt. Polytechnic College, Kannur, Kerala.

Abstract:
Steel-to-aluminum joints are now used to reduce transportation costs and fuel consumption. These joints are used in industries ranging from nuclear, aerospace, and naval to automobile and kitchen. According to previous research, fusion welding processes are not appropriate for these joints; instead, solid-state welding, particularly friction stir welding, is an appropriate method to use for these joints. However, using this method for these two metals requires accurate temperature distribution and material flow prediction in order to achieve improved joints. The Level Set (LS) method was used to perform a morphological simulation of the weldment. The temperature distribution and material flow velocity during the welding process were calculated using thermal and computational fluid dynamics (CFD) simulations. Based on the CFD results, a level set model was developed to predict weld morphology. Weld morphologies were simulated at various tool rotational speeds, offset positions, and specimen height levels. Temperature measurements, optical microscopy (OM) of the weldment, and scanning electron microscopy (SEM) of the stirred zone (SZ) were performed to validate the simulations. Steel particles detached in the aluminium matrix were discovered to be the primary cause of defects in the weld zone. According to the simulation results, increasing the rotational speed and offset through the steel side could result in more steel particles.

Keywords: *Weld Morphology, Dissimilar joint, Friction stir welding, Aluminum- Stainless Steel Joint, Morphology, simulation, Level set method.*

I. Introduction:

Friction stirs welding (FSW), a type of solid-state welding method, is appropriate for joining aluminium alloy to stainless steel. It should be noted, however, that the quality of these welds is dependent on the distribution of steel particles in the aluminium matrix in the stir zone (SZ). Dehghani et al. (2013) [1] investigated defects caused by FSW of Al to steel and discovered that welding parameters and tool geometry have a significant effect on defect reduction. Investigating material flow during FSW greatly assists engineers in controlling aluminium to steel welding parameters and achieving better welding results. Lorrain et al. (2010) [2] compared different tool shapes to investigate material flow during FSW of reinforced aluminium alloys. Their investigations revealed a low vertical motion of material flow towards the weld zone's bottom. Seidel and Reynolds (2011) investigated material transport in the stir zone using a semi-quantitative approach and experimentally studied FSW material flow using the marker insert technique. [3]

The level set method (LS) has been proposed as a suitable mathematical and numerical method for predicting two-phase flow morphology by computing changes in physical properties of materials at the moving interface between two materials. This method was developed by Osher and Sethian (1988) to simulate fluid flow with curvature dependent speed in surface motion problems. Mulder et al. (1992) later used this method to simulate gas dynamics. In fact, this method is used to track the interface between two dissimilar materials as they flow through each other. Doefler (2008) demonstrated a CFD model for FSW of various aluminium alloys. [4-5]

Heat transfer model

The temperature field during welding is forecasted using Eq. (1), which is consistent with the Fourier equation.

$$\rho\, C\, p\, u\, (\nabla T) = \nabla(k\, \nabla T) + Q \qquad \ldots\ldots\ldots\ldots\ldots\ldots \quad (1)$$

In this equation, k represents thermal conductivity (W/m^3), Cp represents heat capacity (J/kg K), p is the material density (kg/m^3), u represents the velocity field from CFD calculations, and Q (W/m^3. s) represents the generated heat rate. For the heat generation tool in FSW, a steady-state analysis was used, and translational motion was assumed. Song and Kovacevic (2006) used a similar method for thermal simulation of the FSW process previously. [6]

Level Set method

To predict the morphology of the weld zone, a 2D model was created and LS equations were solved in the 2D domain. Although the CFD simulations were performed in 3D domain, this simplifying step was used due

to the large number of calculations required for importing and solving the 3D equations in LS method and the limitations of our computational facilities. In fact, weak coupling was used, and the local physical properties of the mixed zone do not depend on the local composition. It should be noted that this is clearly one of the model's limitations, and for more accurate results, the 3D LS model is preferred. [7]

II. Review of Literature:

Shuai Zhang et al. [8] designed a CFD prototypical with a geometrical prototypical and a fragmented contact limit situation to investigate the effects of hardware tilt edge continuously on the in-process heat move and mass exchange during FSW. The creator discovered three promising outcomes. First, the slope welding instrument produced a higher temperature on the propelling crosswise, which is attributed to the fragmented interaction at the shoulder/work piece boundary. Second, the slope welding instrument generates more frictional power at the device/work piece interface, allowing the interfacial material stream speed to be recovered after the device. Third, the slope welding apparatus generates a more grounded blending activity towards the substantial in the vicinity of the fusing instrument, which is beneficial for material blending and the development of grating mix welds.

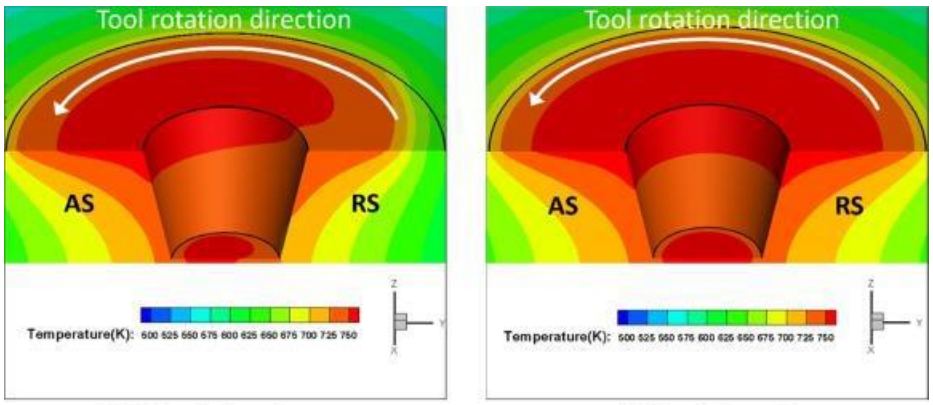

(a) 2.5° tool tilt angle (b) 0° tool tilt angle

Figure 3 Effect of Tilt angle on heat transfer during FSW process [8]

Experimental work

The experimental FSW was used to validate the simulations for two plates of 304 SS and AA-5083 with the compositions shown in Tables (1) and (2). The specimens were 150×60×3 mm in length. As shown in Fig. 3, two K-type thermocouples were planted 1.5mm deep with the specimens near the shoulder, 9mm for SS and 11mm for Al distance from the centre line. To reduce the air gap and obtain more accurate measurements, the thermocouples were pressed into the holes of both materials (Fig. 3). [9]

Table 1: Chemical composition of 304 SS.

C	Mg	P	S	Si	Cr	Ni	N
0.08	0.2	0.045	0.03	0.75	18	9	0.1

Table 2: Chemical composition of AA-5083.

Si	Fe	Cu	Mn	Mg	Cr	Zn	Ti
0.4	0.4	0.5	0.6	4.5	0.08	0.25	0.15

For welding, a WC-Co tool with a shoulder radius of 9mm, an average pin radius of 3mm (a 4mm to 2mm cone), and a pin height of 2.7mm was used. According to Fig. (3), a 1mm offset towards the Al side was used to reduce the entry of rough steel particles in the Al matrix in the stir zone (SZ). The normal force used during welding was 30kN, and the welding was done at different rotational speeds of 350, 500, and 700 RPM with an 80 mm/min velocity. Temperature measurements were taken at 40 and 80 mm/min velocities with a rotating speed of 500 RPM. [10]

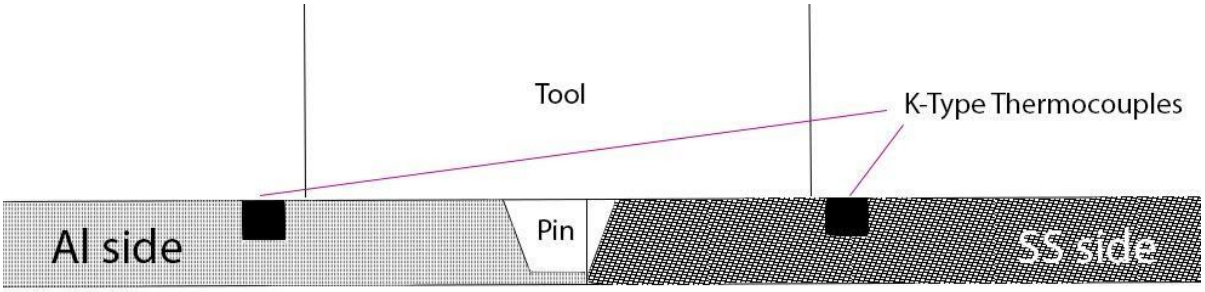

Figure 3. Schematic cross section of weld with offset through aluminum side and thermocouples positions.

III. Result and Discussion:

Weld morphology evaluation

Simulation results for various conditions were used to evaluate the morphology of the stirred zone. In this study, the LS simulation time was set to 1 second. In fact, the translational motion velocity was 80 mm/min, or 1.33 mm/s, for all simulations and experiments. That means the pin moves 1.33 mm in the joint length direction in 1 second of simulation time. Furthermore, the pin rotation during this time (1 sec.) ranges from 5.8 to 11.6 RPS, yielding reasonable results for stirred weld morphology.

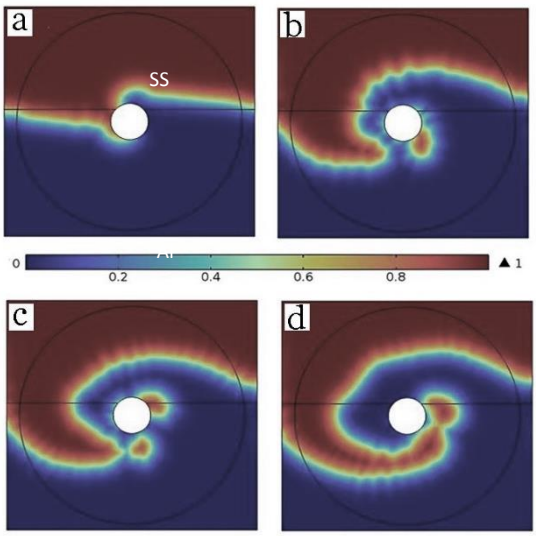

Ø

Figure (12) depicts the phase distribution of two materials in the middle section at various times of rotational speed of 350 RPM, namely 0.1, 0.5, 0.7, and 1 second. It can be seen that there is a flow from the steel side to the aluminium side at the start of the stirring process. [11]

The effects mentioned above can be verified using a metallographic image of a transversal cross section of welded specimens at various rotational speeds, as shown in Fig. (15). This figure clearly shows that as the rotational speed increases, the steel penetration into the aluminium side becomes more severe. Figure (15 d) depicts a horizontal slice of the weldment at the end of the welding process, when the tool was pulled out of the specimen. The flow of steel through the Al side is visible in this figure. This figure also shows steel particles that became detached from the base due to the higher rotational speed.

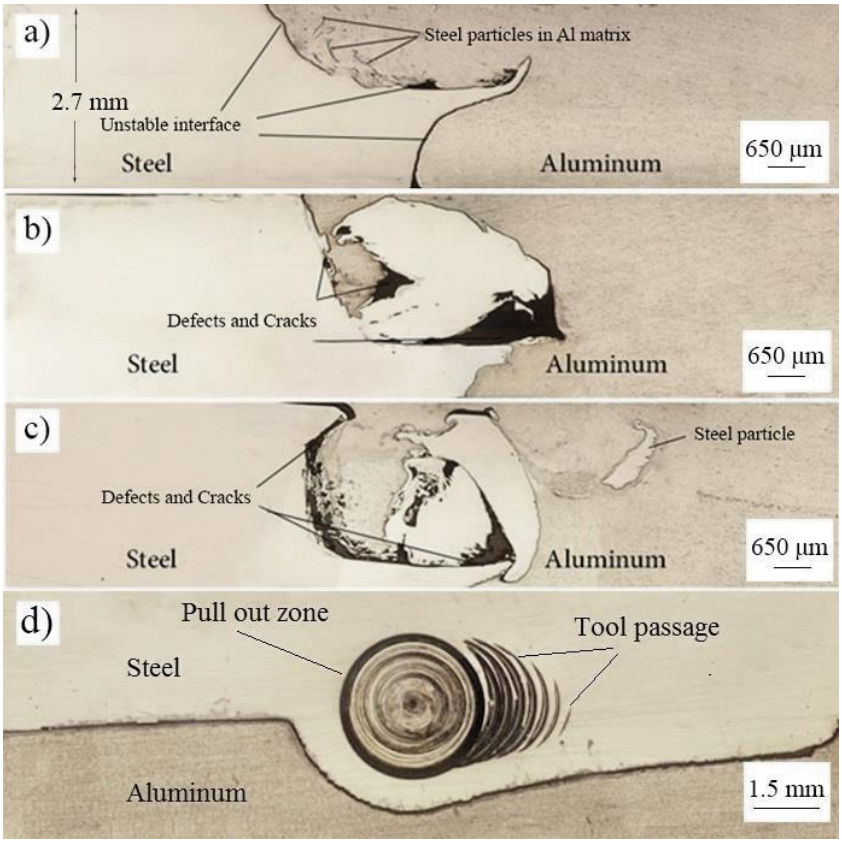

Figure 15. Metallographic image of transversal cross-section of welded zone in different rotational speed: a) 350 RPM, b) 500RPM, c) 700 RPM and d) Horizontal slice of the weld polished at ½ of height in the tool pull out zone. [12-13]

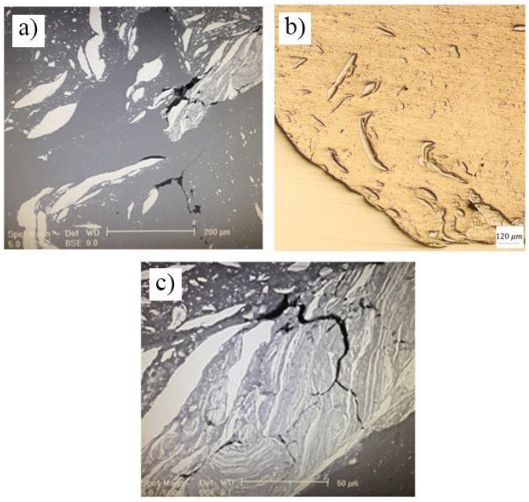

Figure 17. Metallographic figures, a) SEM figure of steel particles in aluminum matrix, b) Optical microscopy of steel particles inaluminum matrix, c) crack propagation beside steel particle. [14-15]

IV. Conclusion:

Thermal and CFD simulations were used in this study to simulate flow velocity during welding, and an LS model was created to simulate weld morphology. The distribution of steel particles in the SZ is the primary cause of problems and defects during dissimilar FSW of Al to SS. Thermal and CFD models revealed that the SS side has higher viscosity, implying that having hard particles can cause crack initiation during welding.

References:

[1]. Dehghani, M., Amadeh, A. & Mousavi, S. A. 2013. Investigations on the effects of friction stir welding parameters on intermetallic and defect formation in joining aluminum alloy to mild steel. Materials & Design, 49, 433-441.

[2]. Lorrain, O., Favier, V., Zahrouni, H. & Lawrjaniec, D. 2010. Understanding the material flow path of friction stir welding process using unthreaded tools. Journal of Materials Processing Technology, 210, 603-609.

[3]. Seidel, T. & Reynolds, A. P. 2001. Visualization of the material flow in AA2195 friction-stir welds using a marker insert technique. Metallurgical and materials transactions A, 32, 2879- 2884.

[4]. Mulder, W., Osher, S. & Sethian, J. A. 1992. Computing interface motion in compressible gas dynamics. Journal of Computational Physics, 100, 209-228.

[5]. Mulder, W., Osher, S. & Sethian, J. A. 1992. Computing interface motion in compressible gas dynamics. Journal of Computational Physics, 100, 209-228.

[6]. Song, M. & Kovacevic, R. 2003. Thermal modeling of friction stir welding in a moving coordinate system and its validation. International Journal of Machine Tools and Manufacture,43, 605-615.

[7]. Dörfler, S. M. Advanced modeling of friction stir welding–improved material model for aluminum alloys and modeling of different materials with different properties by using the levelset method. Proceedings of the COMSOL 2008 Conference, COMSOL, Hannover, 2008.

[8]. Zhang, S., Shi, Q., Liu, Q., Xie, R., Zhang, G. and Chen, G., 2018. Effects of tool tilt angle on the in-process heat transfer and mass transfer during friction stir welding. International Journal of Heat and Mass Transfer, 125, pp.32-42

[9]. Liu, X., Lan, S. & Ni, J. 2014. Analysis of process parameters effects on friction stir welding of dissimilar aluminum alloy to advanced high strength steel. Materials & Design, 59, 50-62.

[10]. Nandan, R., Roy, G. & Debroy, T. 2006. Numerical simulation of three-dimensional heat transfer and plastic flow during friction stir welding. Metallurgical and materials transactions A, 37, 1247-1259

[11]. Tomashchuk, I., Sallamand, P., Jouvard, J. & Grevey, D. 2010. The simulation of morphology ofdissimilar copper–steel electron beam welds using level set method. Computational Materials Science, 48, 827-836.

[12]. Colegrove, P. A. & Shercliff, H. R. 2005. 3-Dimensional CFD modelling of flow round a threaded friction stir welding tool profile. Journal of Materials Processing Technology, 169, 320-327.

[13]. Liu, X., Lan, S. & Ni, J. 2014. Analysis of process parameters effects on friction stir welding of dissimilar aluminum alloy to advanced high strength steel. Materials & Design, 59, 50-62.

[14]. Piccini, J.M.; Svoboda, H.G. Tool geometry optimization in friction stir spot welding of Al-steel joints. J. Manuf. Process. **2017**, 26, 142–154.

[15]. S. Ragu Nathan, V. Balasubramanian, S. Malarvizhi, and A. G. Rao, "Effect of welding processes on mechanical and microstructural characteristics of high strength low alloy naval grade steel joints," *Defence Technology*, vol. 11, no. 3, pp. 308–317, 2015.